Terahertz Diode on AlGaN Microcathode

N.M. GONCHARUK

Research Institute "Orion", Egena Potie 8a, 03680 Kiev, Ukraine
Tel.: 38(044)4566071

Abstract. This paper deals with small-signal model of diode on base of electron field emission of AlGaN microcathode and electron transit in vacuum layer, which width is less than one micron. Electron emission delay time dependent on Al fraction in cathode is comparable with transit time and less than a picosecond for the diode.

Therefore we have included consideration of the emission delay when studying diode impedance characteristics. The investigations show that diode negative conductance spectrum being single-band or multiband depending on a ratio of emission delay time to alternating signal period is in terahertz frequency range. Maximal value of negative conductance in the spectrum and frequency of the maximum are the more than less emission delay time value.

1. Introduction

Negative conductance of available microwave semiconductor barrier-injection transit-time (BARITT) diode is a result of the electron transit delay effect alone because of negligible small electron injection delay time as compared with electron transit time. We have modified BARITT diode small-signal theory [1] to investigate vacuum barrier-emission transit-time diode on base of electron field emission of *AlGaN* microcathode and electron transit in vacuum. Time of electron tunneling under potential barrier of electron affinity energy in the emitter is comparable with transit time for the studied diode. Therefore in the small-signal model of the diode we unlike Sze [1] take into account delay both transit and emission as for a single-barrier diode in [2]. In addition an acceleration of electron in transit layer has been included into consideration as distinct from supposed in [1] and [2] constancy of electron drift velocity.

2. Model Description

Active layers of the diode studied are a layer of *AlGaN* emitter, a vacuum layer of potential barrier of electron affinity energy in the emitter and a vacuum transit layer. Fig. 1 shows energy diagram of the diode studied.

Time-independent current density of electron field emission is expressed as

$$J = A\int_0^{\infty} T_V \ln\left|1+\exp\left[\left(e_f - e_z\right)/ k_B T\right]\right| \mathrm{d}e_z \qquad (1)$$

here $A = 4\pi q m_c m_e {}^* k_B T/h^3$, q and m_e^* are electron charge and effective mass in emitter, m_c degeneracy of emitter conduction band, k_B and h are Boltzmann and Plank's constants, e_f and e_z are Fermi energy and emitter electron energy component perpendicular to emitting surface, T is diode temperature and T_V permeability of the potential barrier for an emitted electron.

A tunnel resistance of the potential barrier is inverse to derivative of a current density on voltage. It is expressed for the diode as $r_t = b/\sigma$, where $\sigma = dJ/dF$ is positive differential emission conductivity of the diode. F is constant electric field in vacuum and b is potential barrier width for emitted electron which energy we suppose equal Fermi energy. At this assumption $b = (\chi - \varphi_s - e_f)/qF$ where χ and φ_s are the electron affinity energy and emitter conduction band bending on boundary with the barrier. Time of electron tunneling under the potential barrier $\tau_t = r_t c_t = \varepsilon_0/\sigma$, where $c_t = \varepsilon_0/b$ is barrier layer capacitance per unit area, ε_0 vacuum permittivity constant.

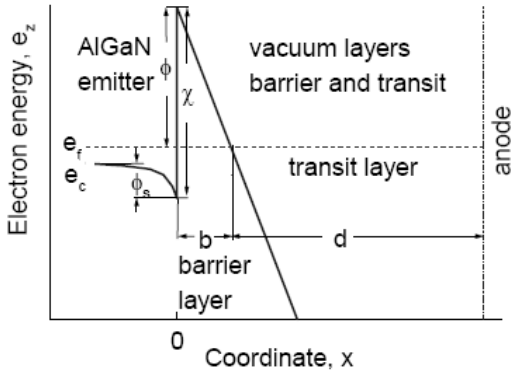

Fig. 1. Energy diagram of the diode.

Diode microwave impedance is calculated in framework of small-signal model like the same one developed by Sze [1] for BARITT diode but involving electron emission delay and acceleration of electron in vacuum transit layer. Expressions for active and reactive components of the impedance derived neglecting emitter conduction band bending are the following

$$r = a\left(a_1\cos\varphi - a_2 b_2\right)/ z_1 + b\cos\varphi/\sigma z_2 + r_s \qquad (2)$$

$$x = a\left(a_2\cos\varphi - a_1 b_1\right)/ z_1 - bb_2\ /\sigma z_2 - 1/\omega c_d \qquad (3)$$

here $a = u\sigma/\omega^4\varepsilon_0^2$, $a_1 = \cos\theta + \theta\sin\theta - 1$, $a_2 = \theta\cos\theta - \sin\theta$, $b_1 = 1/\varphi - \sin\varphi$, $b_2 = \varphi - \sin\varphi$, $z_k = \cos^2\varphi + b_k^2$, $\omega = 2\pi f$, f is alternating signal frequency, τ and $\theta = \omega\tau$ are time and angle of electron transit, $\varphi = \omega\tau_t$ is emission delay angle, $u = qF/m_0$ and m_0 are acceleration and mass of electron in vacuum transit layer, $c_d = \varepsilon_0/d$ is transit layer capacitance, $d = u\tau^2/2$ transit layer width, $r_s = \rho_c + \rho_e l_e$ is diode parasitic series resistance in absence contact spreading resistance, ρ_c contact specific resistance, ρ_e and l_e are resistivity and total width of semiconductor epitaxial layers of the diode.

3. Analysis of Numerical Calculation Results

Numerical calculations were conducted for three diodes with presented in Table 1 values of electron affinity energy in emitter which correspond with different values of *Al* fraction x in $Al_xGa_{1-x}N$ emitter. We suppose diode temperature 300*K*, an emitter doping level $5\cdot10^{18}$ cm^{-3} and the following parameters of the parasitic resistance $l_e = 250$ nm, $\rho_e = 10^{-3}$ Om×cm, $\rho_c = 10^{-7}$ Om×cm^2 [3].

Table 1. Diode Parameters And Emission Characteristics

Diode number	Electron affinity energy in emitter (eV)	Electric field (kV/cm)	Minimal tunneling time (ps)
1	0.18	$1.9\ 10^3$	$6\ 10^{-2}$
2	0.44	$6.5\ 10^3$	$2.5\ 10^{-1}$
3	0.61	$1.04\ 10^3$	$6\ 10^{-1}$

Dependences of differential emission conductivity on direct electric field in vacuum calculated for the diodes with the above mentioned values of potential barrier of electron affinity energy in emitter are shown in Fig. 2. The emission conductivity reaches maximum which value is the more and the maximum is reached at the less electric field value than the potential barrier is lower. Table 1 shows values of electric field and minimal emission delay time which correspond with the emission conductivity maxima for the diodes.

Microwave impedance characteristics per unit of diode cross-section area computed for the diodes with the minimal values of emission delay time are shown in Fig. 3–5. When analyzing the impedance characteristics it is seen that negative conductance spectra of all the diodes are in terahertz frequency range. The spectrum is singleband or multiband depending on frequency inverse to tunneling time is higher or lower than upper frequency of diode negative conductance frequency spectrum.

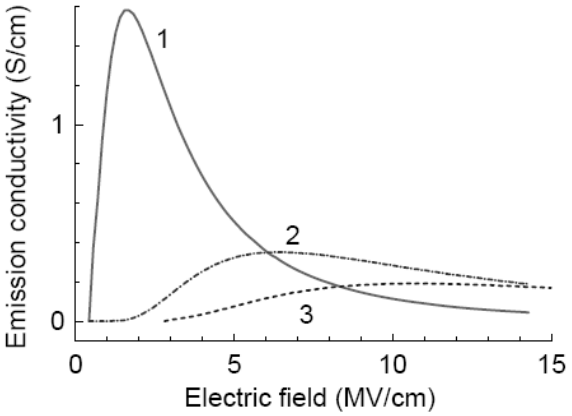

Fig. 1. Differential emission conductivity dependences on direct electric field in vacuum for the diodes with the electron affinity energy in emitter 0.18 eV, 0.44 eV, 0.61 eV.

Tunneling time is less than alternating signal period at all frequencies in negative conductance spectrum of the diode 1 so the spectrum is single-band. For the diodes 2 and 3 a ratio of tunneling time to alternating signal period is less than unit in lower part of negative conductance spectrum and it is more than unit in upper part of the spectrum. When frequency in the spectrum changes value and sign of the greatest first term in (2) oscilate due to oscilations included into it periodical functions of emission delay angle. The angle increases to about 0.9π, 5π and 11π when frequency increases to upper limits in the spectra of the diodes 1, 2 and 3 accordingly. This modulation of negative resistance frequency dependence results in multiband spectra of the diodes 2 and 3. Except the basic first band at frequencies less than emission delay frequency $f_t = 1/\tau_t$ additional bands are in the rest upper part of the spectrum.

Fig. 3. Frequency dependences of negative resistance (Fig. 3*a*) and negative conductance (Fig. 3*b*) of the diode 1 at transit angles $\theta = k\pi/5$, where k is curve number. Fig. 3 presents negative resistance and negative conductance frequency dependences for diode 1. There is one peak on every of the two dependences. Value of negative resistance peak increases and frequency of the peak lowers when transit angle increases. A value and frequency of negative conductance peak and a width of negative conductance frequency band depend on a ratio of transit time to tunneling time. When transit angle increases from zero to value of emission delay angle the band appears and broadens as its upper frequency increases and lower frequency decreases, frequency of negative conductance peak increases. When transit angle further increases to 2π frequencies upper and of the peak decrease, the band narrows and lowers. Negative conductance peak value reaches two maxima with transit angles about $\pi/2$ and $3\pi/2$ accordingly and one minimum with transit angle near π. It tends to zero when the transit angle approaches to 2π.

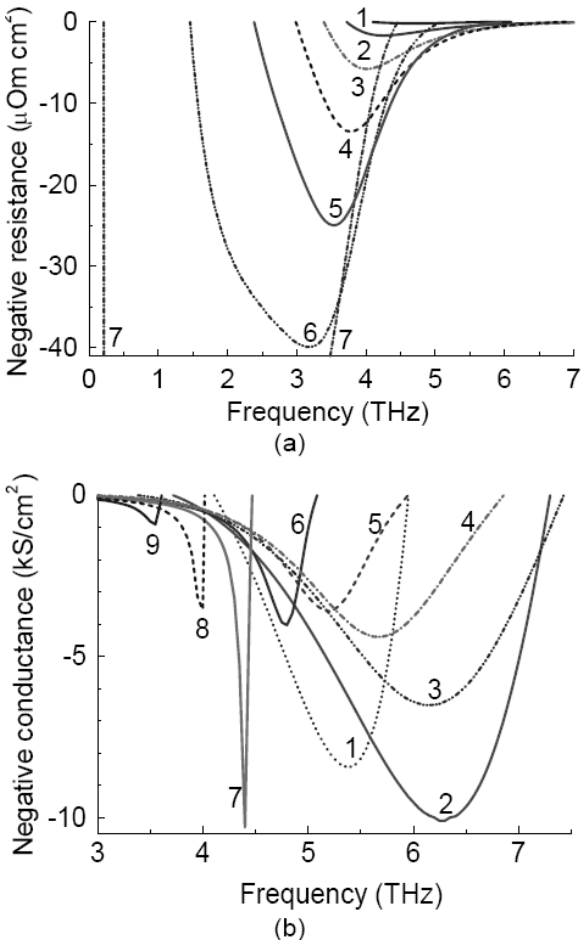

Fig. 3. Frequency dependences of negative resistance (Fig. 3*a*) and negative conductance (Fig. 3*b*) of the diode 1 at transit angles $\theta = k\pi/5$, where k is curve number.

Frequency dependences of negative resistance of the diode 2 at frequencies of the lowest first band are shown in Fig. 4a and at frequencies in the rest upper part of the spectrum in Fig. 4b. Two additional bands of negative resistance take place at frequencies near emission delay frequency and doubled this frequency accordingly. A value of negative resistance peak in a band increases and frequency of the peak decreases with transit angle increasing. A value of negative resistance peak in the basic first band is three orders more than the same one the second additional band.

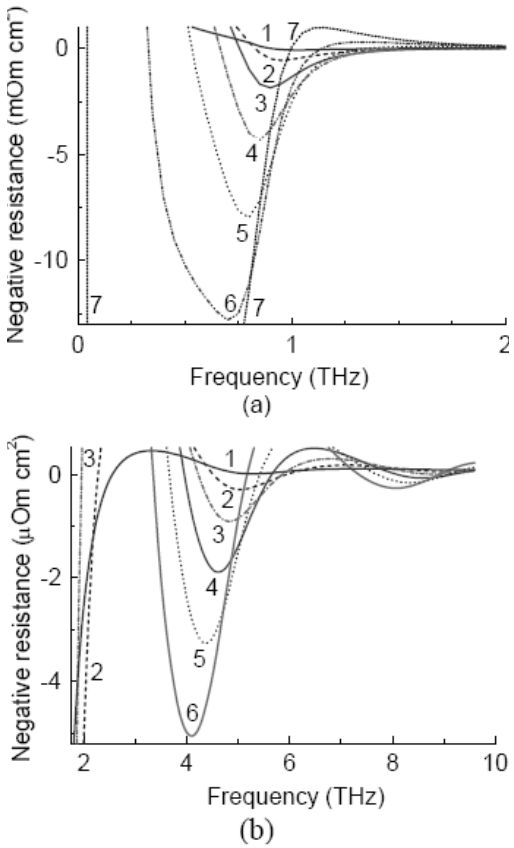

Fig. 4. Frequency dependences of negative resistance for the diodes 2 in lower (Fig. 4*a*) and upper (Fig. 4*b*) part of negative conductance frequency spectrum at transit angles $\theta = k\pi/5$, k is curve number.

Analysis of negative conductance multiband spectra the diodes 1 and 2 in Fig. 5 shows the more transit angle the lower frequency bands of negative conductance in the spectra. Maximal peak of negative conductance in a band takes place at transit angle near the least its value in the band. However lower limit of transit angle interval where negative conductance is present in a band increases with band number increasing. Therefore the transit angle corresponding with maximal negative conductance in band is the more than the band is higher. For both the diodes the greatest peak in the first band takes place near half of emission delay frequency and transit angle of $\pi/4$. When tunneling time increases the negative conductance spectrum widens; bands narrow and increase in the number; value, frequency and transit angle corresponding with the greatest peak in the spectrum decrease.

Admittance reactive component at frequency of the greatest negative conductance peak is comparable with the same active component for the diode 1 and of one order more for the diodes 2 and 3. Its value decreases with emission delay increasing.

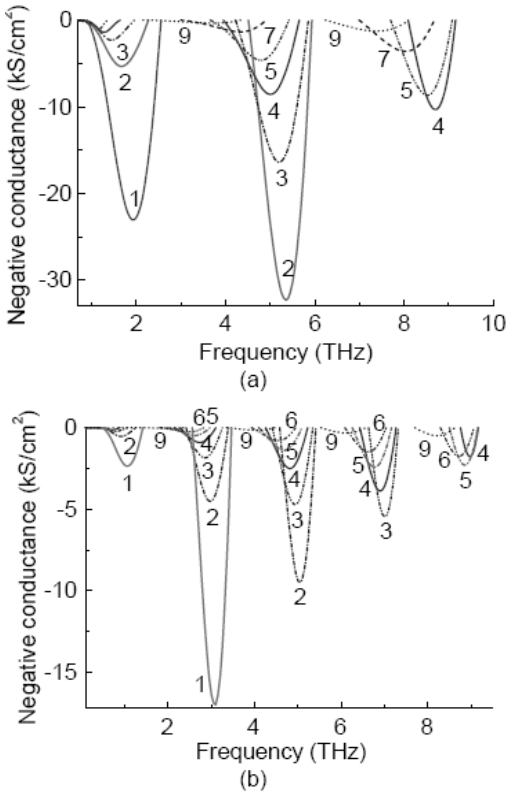

Fig. 5. Frequency dependences of negative conductance for the diodes 2 (Fig. 5*a*) and 3 (Fig. 5*b*) at transit angles $\theta = k\pi/5$, *k* is curve number.

Transit layer width values at frequencies of the greatest negative conductance peaks shown in Fig. 3b, 5a, 5b are close to 17 nm and 420 nm for the diode 1 with transit angles $\pi/2$ and $3\pi/2$, 80 nm and 950 nm for the diodes 2 and 3 with the angle $\pi/2$ and $\pi/4$ accordingly.

4. Conclusion

Terahertz frequency spectrum of negative conductance of the diodes is single-band or multiband depending on emission delay frequency is more or less than upper frequency in the spectrum. Modulation period of negative resistance

multiband spectrum is near emission delay frequency. The first negative conductance band in the spectrum is near one half of emission delay frequency. The less is emission delay time the more value, frequency and transit angle corresponding with the greatest peak of negative conductance in the spectrum. Advantage of the diode over semiconductor the same one [2] is higher operating frequency due to less barrier width which value is into interval from 0.9 nm to 0.6 nm for the diodes.

References

[1] S.M. SZE, *Physics of Semiconductor Devices*, **2**, Chapter 10, Section 7, New York: J. Wiley & Sons, 1981.

[2] N.M. GONCHARUK, S*ingle-Barrier Diode with Tunnel Injection*, in Proceedings of the 11th International Symposium on RF MEMS and RF Microsystems, MEMSWAVE 2010, Otranto, Italy, June 28-30, 2010.

[3] Q.Z. LIU, S.S. LAU, *A review of the metal-GaN contact technology*, Solid-State Electronics, **42**(5), pp. 677–691, 1998.